Ion sound wave packets at the quasiperpendicular shock front

M. Balikhin,[1] S. Walker,[1] R. Treumann,[2] H. Alleyne,[1] V. Krasnoselskikh,[3] M. Gedalin,[4] M. Andre,[5] M. Dunlop,[6] and A. Fazakerley[7]

Received 15 September 2005; revised 3 November 2005; accepted 14 November 2005; published 28 December 2005.

[1] Electric field measurements from a single spacecraft have been used to study ion-sound turbulence observed within the Earth's bow shock. The observed frequency of the ion-sound waves can be both lower and higher than the local electron cyclotron frequency depending upon the direction of wave propagation in the plasma rest frame. The ion-sound waves observed upstream of the ramp can not be generated either by an instability related to the gradient in the electron temperature or an electric current within the ramp. A comparison of wave vectors for distinctive wave packets indicate that non-stationary, short scale current layers formed in the processes of the ramp evolution might be the source of the free energy for such waves. **Citation:** Balikhin, M., S. Walker, R. Treumann, H. Alleyne, V. Krasnoselskikh, M. Gedalin, M. Andre, M. Dunlop, and A. Fazakerley (2005), Ion sound wave packets at the quasiperpendicular shock front, *Geophys. Res. Lett.*, *32*, L24106, doi:10.1029/2005GL024660.

1. Introduction

[2] The rapid changes that are observed in the plasma at the front of a supercritical, quasi-perpendicular shock lead to the creation of multiple free energy sources for various plasma instabilities. Twin satellite missions, such as ISEE or AMPTE, have provided data for a number of comprehensive surveys of the waves observed in the frequency range (10^{-2}–10^{1} Hz) of the plasma turbulence encountered at the shock front. The use of multisatellite data for wave identification and turbulence studies is limited to the analysis of those waves whose coherence lengths are of the same order of magnitude as the satellite separation distance. Plasma wave modes such as the ion-sound or Lower-Hybrid (LH), that may play an important role at the shock front, possess coherence lengths that are very short in comparison with any realistic satellite separation distance [*Smirnov and Vaisberg*, 1987]. For many of these waves the coherence length is either comparable to or a few times greater than their wavelength. In such cases the waves observed by different satellites in a multisatellite mission will be uncorrelated. This will make it impossible to apply wave identification methods based on intersatellite phase delays [*Balikhin et al.*, 1997a, 2003] or k-filtering. Nevertheless the identification of waves with short wavelengths and the study of their dynamics remains very important because of their potential role in the transfer of energy associated with the upstream directed motion into other degrees of freedom. In the classical model of a quasiperpendicular low β shock anomalous resistivity occurs due to ion-sound turbulence in the shock front [*Galeev*, 1976]. LH waves also may play an important role at the shock front since they can be involved in resonance interactions both with electrons and ions and so are extremely effective at channelling the energy between the two spieces. In order to assess the importance of ion-sound, LH and other waves with relatively short wavelengths within the plasma dynamics of the shock front the mode of the observed waves should first be identified. The strong Doppler shift that results from the large values of $|k|$ precludes the reliable use of the observed frequency for reliable identification as was done in many previous studies. In the present paper it is shown how data from a single spacecraft can be used to determine propagation modes of waves observed in the frequency range 10^{2}–10^{4} Hz at the front of the terrestrial bow shock. A similar approach has been used by *Tjulin et al.* [2003] in a study of lower-hybrid waves in the inner magnetosphere.

[3] The data used in this study were collected by the Cluster EFW instrument on board satellite 3 on February 26th, 2002 at around 2134 UT. At this time, the Cluster satellites were situated at a position (12.1,2.5,8.05) R_e GSE in the foot region of a quasiperpendicular shock ($\theta_{Bn} \sim 55°$, $M_a \sim 4.3$). During this period the EFW instrument onboard Cluster 3 was triggered to operate in internal burst mode for a few seconds. In this particular mode the four individual EFW probe potentials were sampled at a rate of 9000 Hz making it possible to calculate two sets of two parallel electric field vectors. For example, the electric fields E_{31} and E_{24} are computed from the probe differences $P_3 - P_1$ and $P_2 - P_4$ respectively. Both of these electric field measurements lie in the same direction and have a perpendicular separation of ~62.2 m in the direction P_2 to P_3. The availability of two closely spaced, simultaneous measurements enables the use of phase differencing techniques [*Balikhin et al.*, 1997a] to be used for the identification of propagation modes for waves with coherence lengths down to a few Debye lengths based upon single satellite measurements. Since there is no component measured normal to the spin plane, the separation between temporal and spatial variations is possible only in the spacecraft spin plane. As a consequence, phase differencing methods are limited to the determination of the projection of the dispersion in the spin plane. In most cases, however, this can provide enough information to identify the plasma wave mode. This approach is implemented in the present study. Plasma mea-

[1]Automatic Control and Systems Engineering, University of Sheffield, Sheffield, UK.
[2]Max-Planck-Institute for extraterrestrial Physics, Garching, Germany.
[3]Laboratoire de Physique et Chimie de l'Environnement, CNRS, Orleans, France.
[4]Department of Physics, Ben-Gurion University, Beer-Sheva, Israel.
[5]Swedish Institute of Space Physics, Uppsala, Sweden.
[6]Space Sciences Division, Rutherford Appleton Laboratory, UK.
[7]Mullard Space Science Laboratory, Department of Space and Climate Physics, University College London, London, UK.

0094-8276/05/2005GL024660

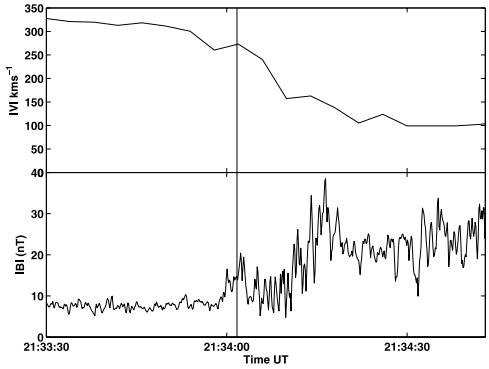

Figure 1. The (top) magnitude of the magnetic field and (bottom) ion bulk flow measured during the shock crossing that occurred on February 26th, 2002 at 2134 UT.

surements were obtained from the CIS HIA (ions) and PEACE (electron) instruments. Magnetic field data were obtained from FGM. It should be noted that the spin vector of the Cluster satellites is almost coincident (to within 5°) with the −Z GSE axis.

2. Observed Waves

[4] The ion bulk velocity and the magnitude of the magnetic field as measured by Cluster 3 spacecraft are plotted in Figure 1. Initially, the spacecraft was in the solar wind. The foot region was encountered just before 2134 UT and the shock ramp was crossed around 2134:12.5 UT. The plasma bulk velocity began to decrease around 2133:50. Shortly before 2134 low frequency oscillations were observed in the magnetic field, a feature commonly observed in the foot region of supercritical shocks. The beginning of the foot region is characterised by a nonlinear structure similar to the S-structures previously reported by *Walker et al.* [1999]. A comparison of magnetic field and plasma data show that this S-structure is not a partial penetration of the ramp. The present study is limited to the short interval at the beginning of the internal burst mode indicated by the vertical line and coincides with the foot region.

[5] The electric field component E_{31} as measured during the initial part of the internal burst mode interval is shown in Figure 2 (top) and its Morlet wavelet spectra is shown in

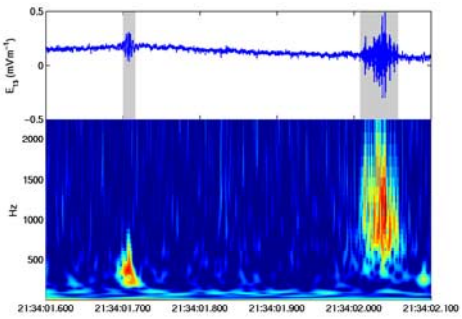

Figure 2. The (top) waveform and (bottom) wavelet spectrogram of the electric field computed from the difference in potential between probes 3 and 1.

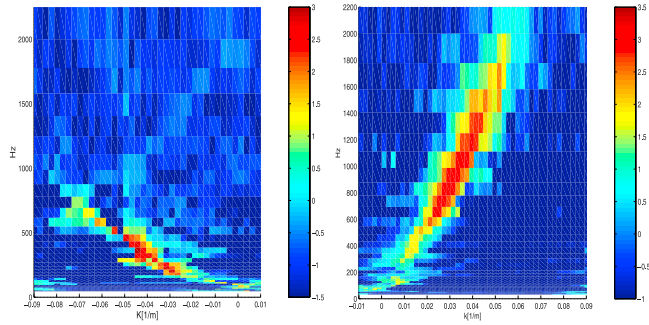

Figure 3. Examples of the $f-k$ spectrograms for the (left) first and (right) second wave packets.

Figure 2 (bottom). The electric field fluctuations show a pair of well defined wave packets centered around 2134:01.6 and 2134:02.05 UT. Their frequency ranges are 100–800 Hz and 250–2000 Hz respectively. This study will concentrate on the identification of these wave packets to illustrate the use of the technique and its results.

[6] The $f-k_{23}$ spectrum, shown in Figure 3 (left), is a histogram representation of the distribution of wave energy in frequency-k space for the first wave packet [*Balikhin et al.*, 1997a]. The $f-k$ spectrum shows a well developed ridge like maxima, the shape of which indicates the wave dispersion relation projected along the k_{23} direction. This result may be combined with a similar dispersion along the k_{13} to yield the wave vector projection in the satellite spin plane.

[7] Since the angle between the spacecraft spin plane and the GSE XY plane is small, we will consider that the projection into the spin plane is the same as that into the GSE XY plane. The projection of the dispersion relation into the GSE XY plane is shown as the solid line in Figure 4 for the (left) first and (right) second wave packets. The observed frequency range of the first wave packet (100–800 Hz) corresponds to approximately $0.25-1.9\omega_{ce}$, where ω_{ce} is the electron cyclotron frequency, and the magnitude of wave vector projection is in the range $0.015 < |k1| > 0.075$ m^{-1}. For this interval the electron temperature is $T_e \sim 17$ eV and plasma density $n_i = 9.7$ cm^{-3}. This leads to an estimate for the Debye length of $\lambda_d \approx 10$ m. Thus the observed values of for the projection k correspond to $\approx 8-40\lambda_d$.

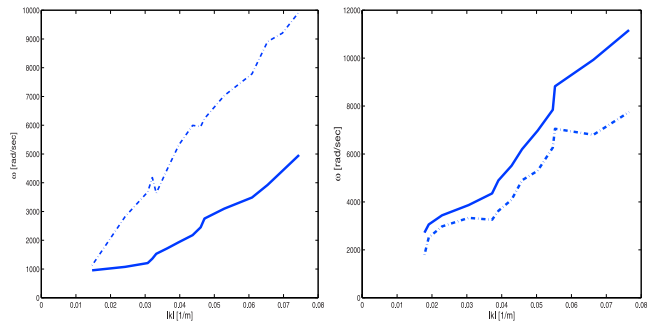

Figure 4. The plasma wave dispersion relation projected into the GSE XY plane for the (left) first and (right) second wave packets. The solid line represents the projection of the dispersion relation whilst the dotted line shows the contribution of the Doppler shift term $k \cdot V_{sw}$.

[8] The satellite frame dispersion relation in the satellite spin plane is shown by the solid line in Figure 4. Its phase velocity is in the range 40–70 kms^{-1}. The Doppler shift can be estimated as the scalar product of the solar wind velocity and spin plane wave vector component. This estimation of the Doppler shift term is shown as a dashed line. It has the same sign as the phase velocity and is always greater than the observed wave dispersion indicating that in the plasma frame the waves propagate in the direction opposite to that of the solar wind, but are convected Earthwards by the plasma flow. This convection reverses the direction of propagation in the satellite frame. The average angle between the spin plane projections of wave vector and the magnetic field is about 20°.

[9] The second wave packet analysed was observed ≈0.3 seconds after the first. The electric field waveforms (not shown) again indicate a good correlation between the corresponding electric field components measured by different probe pairs. The $f - k_{23}$ spectrum calculated for this wave packet is shown in Figure 3 (right). The ridge like maxima in these spectra correspond to the projections of the wave dispersion relation in the direction k_{23}. The resulting dispersion relation is shown as the solid line in Figure 4 (right). Its frequency range is 250–2000 Hz (≈0.6–4.9ω_{ce}), and the magnitude of wave vector projections is in the range ≈0.018–0.075 m^{-1}. For this wave packet, the satellite frame phase velocity is in the range 150–160 kms^{-1}. The range of wave vectors and angle of propagation with respect to the magnetic field for the second wave packet coincide with those determined for the first. Even more surprising is the fact that the angle between the two wave vector projections is less than 5°. The dashed line in Figure 4 (right) shows the estimation of the Doppler shift. It can be seen that the Doppler shift term for the second wave packet is less than that of the observed frequency and so the second wave packet propagates in the same direction in both the satellite and plasma frames. Therefore the first and second wave packets propagate in opposite directions in the plasma frame. While for the second wave packet the satellite frame phase velocity is the sum of its plasma frame velocity and the solar wind convection speed for the first wave packet it is their difference. That explains why in the satellite frame the second wave packet propagates faster than the first one.

3. Discussion

[10] The increased level of electric field fluctuations in the frequency range 10^2–10^3 Hz observed in the vicinity of a quasiperpendicular shock front is usually attributed to either ion-sound or whistler waves. One of the most comprehensive studies of the plasma waves in this frequency range was conducted by *Gurnett* [1985]. It's main conclusion was that waves observed above local electron cyclotron frequency are Doppler shifted ion-sound waves whilst those below are whistler mode waves.

[11] The use of multipoint measurements enable the separation of temporal and spatial variations. In the current study it is possible to distinguish which of these two wave modes was observed. Thus we have a method that is independent of using the observed frequency criterion formulated by *Gurnett* [1985]. For this interval $|B| \sim$ 14.8 nT and hence the local electron cyclotron frequency $f_e \sim 415$ Hz. As can be seen from the $f - k$ spectra shown in Figure 3 that the maximum wave energy of the first wave packet occurs at a frequency lower than f_e. According to the classification used by *Gurnett* [1985] this should be a whistler wave packet whose dispersion relation may be written as (neglecting thermal corrections) $\omega^2 = \omega_e^2 \cos^2\theta_{Bk} k^2 c^2/(k^2c^2 + \omega_{pe}^2)$, where θ_{Bk}, ω_e, ω_{pe} are the angle between the wave vector and the magnetic field, the electron cyclotron and electron plasma frequencies respectively. The wave vectors for the first wave packet lie in the range $kc/\omega^2 \sim 30$–150 and therefore correspond to the electrostatic limit of the mode for which the plasma frame frequency should be $\sim\omega_e \cos\theta_{Bk}$. If we estimate the angle θ_{Bk} using the angle between the projections of wave vector and the magnetic field in the spin plane, the plasma frame frequency can be estimated as $f_e \cos\theta_{Bk} \sim 280$ Hz. For the wavevectors found, $0.015 < k < 0.0075$ m^{-1} the electrostatic whistler phase velocity varies in the range $24 < v_{ph} < 112$ kms^{-1} in the plasma rest frame. In the spacecraft frame the slowest waves would reverse their direction of propagation, so that waves propagating in both directions would be observed. However, it has been shown earlier that all waves are propagating in the same direction. Moreover, for the strongly dispersive electrostatic whistler the phase velocity should vary by a factor of two or more over the observed range of wavevectors, while the actual variation is within 20% only. These arguments exclude the possibility that the observed mode is the whistler in the electrostatic regime.

[12] The other possibility is the ion-sound mode. Since we are limited to spin plane measurements of the wave vectors only order of magnitude estimations of the wave parameters can be made. For such crude calculations we will disregard the factor $\theta_{Bk} \sim 18°$ in the dispersion of ion-sound waves and use the simplified form $\omega = kv_{is}/\sqrt{1 + k^2\lambda_D^2}$ where $v_{is} = \sqrt{k_b T_e/M_i}$ is the ion-sound velocity, and k_b is Boltzmann's constant. During the time interval in which both waves packets were observed $v_{is} \approx$ 40 kms^{-1}. Thus, in the plasma rest frame the wave phase velocity should be in the range $0.80v_{is} < v_{ph.pf} < 0.99v_{is}$. This velocity dispersion is very close to the observations. If the observed waves are indeed ion-sound waves their plasma frame frequency should be in the range ≈75–100 Hz, much lower than the observed frequency. This disagreement can be attributed to the Doppler shifts estimated as $\frac{|k|}{2\pi} V_{sw} \sim 600$–$3000$ Hz. In reality the Doppler shift is smaller due to the angle between the wave vector and the solar wind velocity.

[13] The above arguments indicate that the first wave packet consists of ion-sound waves. As previously mentioned, the wave vectors for the second packet have exactly the same range as the first. Therefore, all arguments used above to deduce the wave mode of the first wave packet are valid for the second. The main difference between these two wave packets is in the sign of the Doppler shift. For the first wave packet, the observed frequency is the difference between the Doppler shift and the plasma frame frequency whilst for the second it is their sum. Not only are the ranges of k similar but also their GSE XY components as shown in Figure 5. It can be seen that they almost coincide for the whole range of observed waves. The angle between

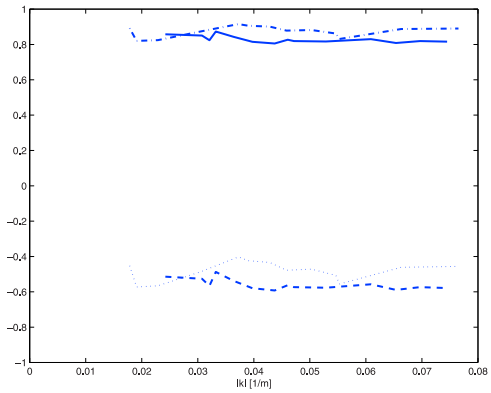

Figure 5. A comparison of the wave vector directions for the two wave packets. The dotted and dashed lines represent the X component of wave vector for events 1 and 2, respectively. The corresponding Y components are shown by the dash-dotted and solid lines.

the averaged propagation directions of these wave packets is <5°. This coincidence in the parameters for these two wave packets, observed at clearly distinct periods of time can only be explained by their simultaneous generation at the same location. The generation of ion-sound waves at the shock front are usually attributed either to electric currents or the strong electron temperature gradients in the ramp. Both waves packets were observed upstream of the ramp and carried by the solar wind flow towards it. Since there appear to be no strong gradients in the electron temperature in the foot these waves are probably generated by electric currents. The very short duration of these waves indicates that the current layer might be localized in space and time. Such small scale current layers have been predicted by a nonstationary model of the shock front [*Krasnosel'skikh*, 1985; *Balikhin et al.*, 1997b; *Walker et al.*, 1999]. In this model the quasiperiodic steepening and overturning of the shock ramp takes place leading to the ejection of a nonlinear whistler wave into the upstream region. The amplitude of these S-structures [*Walker et al.*, 1999] can be comparable to the $|B|$ changes in the ramp itself and will be associated with localised currents responsible for the ion-sound waves.

4. Conclusions

[14] 1. It is shown how electric field measurements can be used to separate between temporal and spatial variations on a single satellite.

[15] 2. Local cyclotron frequency cannot be used to distinguish between whistler and ion sound waves at the front of a quasipendicular shock. Ion sound waves are observed both above and below local cyclotron frequency.

[16] 3. Properties of ion-sound waves observed indicate the existence of short lived localised electric currents that can be the result of shock nonstationarity.

[17] **Acknowledgments.** The work was supported by PPARC. The authors wish to thank I. Dandouras for the provision of CIS ion moments.

References

Balikhin, M. A., T. Dudok de Wit, L. J. C. Woolliscroft, S. N. Walker, H. Alleyne, V. Krasnosel'skikh, W. A. C. Mier–Jedrzejowicz, and W. Baumjohann (1997a), Experimental determination of the dispersion of waves observed upstream of a quasi-perpendicular shock, *Geophys. Res. Lett.*, *24*, 787–790.

Balikhin, M. A., S. N. Walker, T. Dudok de Witt, H. S. Alleyne, L. J. C. Woolliscroft, W. Mier-Jedrzejowicz, and W. Baumjohann (1997b), Non-stationarity and low frequency turbulence at a quasi-perpendicular shock front, *Adv. Space Res.*, *20*, 729–734.

Balikhin, M. A., O. A. Pokhotelov, S. N. Walker, E. Amata, M. Andre, M. Dunlop, and H. S. K. Alleyne (2003), Minimum variance free wave identification: Application to cluster electric field data in the magnetosheath, *Geophys. Res. Lett.*, *30*(10), 1508, doi:10.1029/2003GL016918.

Galeev, A. A. (1976), Collisionless shocks, in *Physics of Solar Planetary Environment*, edited by D. J. Williams, pp. 464–490, AGU, Washington, D. C.

Gurnett, D. A. (1985), Plasma waves and instabilities, in *Collisionless Shocks in the Heliosphere: Reviews of Current Research*, *Geophys. Monogr. Ser.*, vol. 35, edited by B. T. Tsurutani and R. G. Stone, pp. 207–224, AGU, Washington, D. C.

Krasnosel'skikh, V. (1985), Nonlinear motions of a plasma across a magnetic field, *Sov. Phys. JETP*, *62*, 282–293.

Smirnov, V., and O. Vaisberg (1987), Evidence of the nonlinear structure at the bow shock front, in *Collisionless Shocks*, edited by K. Szego, pp. 70–76, Budapest.

Tjulin, A., A. I. Eriksson, and M. André (2003), Lower hybrid cavities in the inner magnetosphere, *Geophys. Res. Lett.*, *30*(7), 1364, doi:10.1029/2003GL016915.

Walker, S. N., M. A. Balikhin, and M. N. Nozdrachev (1999), Ramp non-stationarity and the generation of whistler waves upstream of a strong quasiperpendicular shock, *Geophys. Res. Lett.*, *26*, 1357–1360.

H. Alleyne, M. Balikhin, and S. Walker, ACSE, University of Sheffield, Mappin Street, Sheffield S1 3JD, UK. (h.alleyne@sheffield.ac.uk; m.balikhin@sheffield.ac.uk; simon.walker@sheffield.ac.uk)

M. Andre, IRF-U, P.O. Box 537, SE-751 21 Uppsala, Sweden. (mats.andre@irfu.se)

M. Dunlop, Space Sciences Division, RAL, Didcot OX11 0QX, UK. (m.w.dunlop@rl.ac.uk)

A. Fazakerley, Mullard Space Science Laboratory, Department of Space and Climate Physics, UCL, London RH5 6NT, UK. (anf@mssl.ucl.ac.uk)

M. Gedalin, Department of Physics, Ben-Gurion University, P.O. Box 653, Beer-Sheva 84105, Israel. (gedalin@bgumail.bgu.ac.il)

V. Krasnoselskikh, LPCE, CNRS, 3A, Avenue de la Recherche Scientifique, F-45071 Orlans cedex 2, France. (vkrasnos@cnrs-orleans.fr)

R. Treumann, MPE, Karl-Schwarzschild-Str. 1, P.O. Box 1312, D-85748 Garching, Germany. (rat@mpe.mpg.de)